

# Synthesis and Characterization of Polyethylene Glycol Coated Superparamagnetic Fe<sub>3</sub>O<sub>4</sub> Nanoparticles

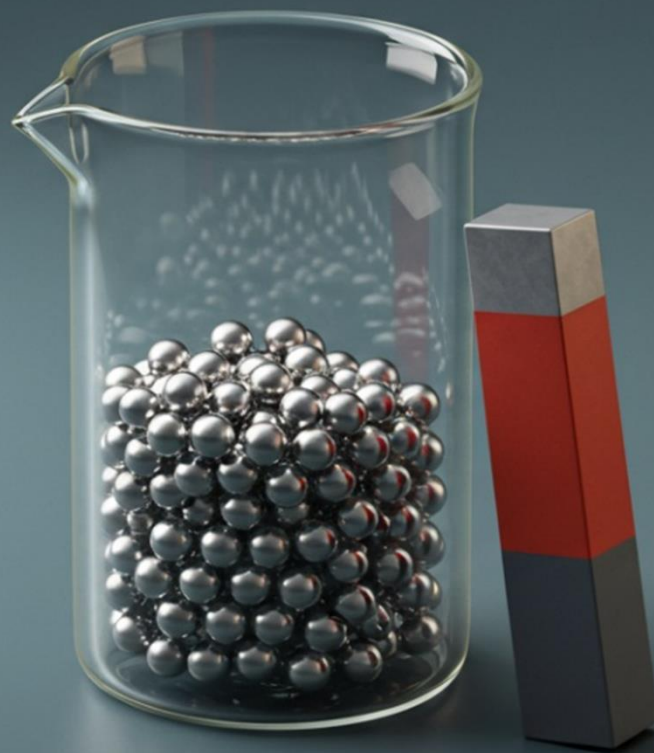
Priyanka A. Patil \*, Shanabhau D. Bagul, Nitesh S. Koche

*Nanomaterials Research Laboratory, Department of Physics, Pratap College Amalner, Maharashtra, India*

**Editor's note:** Superparamagnetic nanoparticles have significant potential for innovative applications across various fields, including material science and engineering, biomedicine, biotechnology, and environmental science. Patil et al. reported that coating iron oxide (Fe<sub>3</sub>O<sub>4</sub>) nanoparticles with polyethylene glycol enhances the performance of these superparamagnetic nanoparticles. The synthesized magnetite Fe<sub>3</sub>O<sub>4</sub> nanoparticles exhibited a cubic inverse spinel structure, had a roughly spherical shape, and were monodispersed. Additionally, Vibrating Sample Magnetometer results demonstrated excellent superparamagnetic behavior and high saturation magnetization at room temperature.

doi: 10.22034/jams.2025.210151

How to cite: P.A. Patil et al. *Journal of Applied Material Science*, 2025, 1, 210151.



JOURNAL OF  
APPLIED  
MATERIAL  
SCIENCE

jams.hsu.ac.ir



## Original Research

# Synthesis and Characterization of Polyethylene Glycol Coated Superparamagnetic Fe<sub>3</sub>O<sub>4</sub> Nanoparticles

Priyanka A. Patil \*, Shanabhau D. Bagul, Nitesh S. Koche

Nanomaterials Research Laboratory, Department of Physics, Pratap College Amalner, Maharashtra, India

### Abstract

The purpose of the present study is to synthesize polyethylene glycol (PEG) coated superparamagnetic iron oxide (Fe<sub>3</sub>O<sub>4</sub>) nanoparticles using a non-toxic, low-temperature, and cost-effective sol-gel method. Fe(NO<sub>3</sub>)<sub>3</sub>·9H<sub>2</sub>O is used as the iron precursor, ethanol as the solvent, and non-toxic triethylamine (TEA) as the gelation agent. Reactions are carried out at a low synthesis temperature of 60°C. The X-ray diffraction (XRD) pattern of the synthesized powder confirmed the magnetite (Fe<sub>3</sub>O<sub>4</sub>) phase of iron oxide with a cubic inverse spinel structure. Field emission scanning electron microscopy (FE-SEM) results confirmed that the resulting Fe<sub>3</sub>O<sub>4</sub> nanoparticles were roughly spherical in shape and monodisperse in nature. Fourier transform infrared spectroscopy (FTIR) results confirmed that the surface of Fe<sub>3</sub>O<sub>4</sub> nanoparticles was coated with PEG through carbonyl groups. FTIR results also showed that the intensity of the band related to the coated powder increased with an increase in the concentration of PEG. The quantitative elemental analysis was done by energy-dispersive X-ray spectroscopy (EDAX). Thermo-gravimetric analysis (TGA) confirmed the presence of PEG in the structure of Fe<sub>3</sub>O<sub>4</sub> nanoparticles. Results of the vibrating sample magnetometer (VSM) showed that the obtained Fe<sub>3</sub>O<sub>4</sub> nanoparticles exhibit excellent superparamagnetic behavior with high saturation magnetization at room temperature. Such superparamagnetic Fe<sub>3</sub>O<sub>4</sub> nanoparticles with a favorable size are promising candidates for biomedical applications.

Keywords: Fe<sub>3</sub>O<sub>4</sub> nanoparticles; PEG coating; Superparamagnetic; FTIR; VSM.

### 1. Introduction

In recent years, nanoscience and nanotechnology have reached great heights to such an extent that it is easy to synthesize, characterize, and control the functional properties of nanomaterials. Nanomaterials possess a great scientific interest because of their outstanding, unique, and beneficial properties [1-4]. Nowadays,

considerable attention has been focused on the magnetic iron oxide nanoparticles (MIONPs) because of their unique properties, such as superparamagnetic, biocompatibility, non-toxicity, etc. They therefore found widespread applications in various disciplines such as material science and engineering, biomedicine, biotechnology, and environmental science.

MIONPs have become a promising candidate for biomedical applications, which include detection and

\* Corresponding author.

Email address: [priyapatil2186@gmail.com](mailto:priyapatil2186@gmail.com) (P.A. Patil)

Received 16 August 2025

Revised 6 September 2025

Accepted 11 September 2025

Available online 14 September 2025

bioseparation of biological entities, magnetic resonance imaging (MRI), Drug delivery systems (DDS), and hyperthermia [5-9]. Several experiments have been carried out on iron oxides, which include  $\text{Fe}_3\text{O}_4$  (Magnetite),  $\gamma\text{-Fe}_2\text{O}_3$  (Maghemite),  $\alpha\text{-Fe}_2\text{O}_3$  (Hematite),  $\beta\text{-Fe}_2\text{O}_3$ ,  $\epsilon\text{-Fe}_2\text{O}_3$ , and  $\text{FeO}$ . Out of these, magnetite and maghemite are the promising candidates for biomedical applications [10].

However, because of the hydrophobic surface and large surface area to volume ratio, MIONPs possess high surface energy, which tends to agglomerate and form large clusters. In order to avoid agglomeration and cluster formation, a suitable coating should be applied on the surface of the MIONPs. Organic polymers, as well as inorganic materials (gold, silica, etc.), are used as coating materials. Polyethylene glycol (PEG) is widely used as a coating material because: (i) it improves the biocompatibility, (ii) it is non-antigenic, (iii) it is non-immunogenic, and (iv) it is water soluble [11-14].

PEG-coated MIONPs can be obtained by many synthesis techniques, such as coprecipitation [15], hydrothermal synthesis [16], electrochemical deposition [17], and thermal decomposition [18]. Among all of these methods, the sol-gel method is widely used because it possesses several advantages such as: (i) it is very simple and cost effective, (ii) it takes place at low temperature, (iii) it controls the stoichiometry of the resultant product, (vi) homogeneous growth of particles with uniform size distribution [19, 20].

In the present study, a two-step synthesis route was used to obtain PEG-coated MIONPs. In the first step, the MIONPs were synthesized, and in the second step, the MIONPs were coated using different amounts of PEG. Characterizations of PEG-coated MIONPs were made by X-ray diffraction (XRD), field emission scanning electron microscopy (FE-SEM), Fourier transform infrared spectroscopy (FT-IR), energy dispersive analysis by X-rays (EDAX), thermogravimetric analysis (TGA), and vibrating sample magnetometry (VSM).

It was observed that the nanoparticles were successfully coated, and magnetic characterization of the nanoparticles showed that the saturation magnetization ( $M_s$ ) of PEG-coated MIONPs was higher than the  $M_s$  value of reported PEG-coated MIONPs [21, 22]. An enhancement of  $M_s$  may make a contribution to the properties of PEG-coated MIONPs and offer improved control over the delivery of nanoparticles for potential applications.

## 2. Experimental

### 2.1. Materials

Chemicals used to synthesize  $\text{Fe}_3\text{O}_4$  nanoparticles were Ferric nitrate ( $\text{Fe}(\text{NO}_3)_3 \cdot 9\text{H}_2\text{O}$ ), ethanol, and triethylamine (TEA). Polyethylene glycol (PEG-6000) was used to coat the surface of  $\text{Fe}_3\text{O}_4$  nanoparticles so as to make them biocompatible. All chemicals used were from Merck Co. and of AR grade.

### 2.2. Synthesis of MIONPs

Ferric nitrate (10.4 mg) was dissolved in 10 ml of ethanol. The solution is stirred under a permanent magnetic stirrer at 350-400 rpm to ensure complete dissolution of the ferric nitrate in ethanol. The temperature of the solution was maintained at 60 °C using a water bath. After complete dissolution, the solution of orange color was obtained. Subsequently, 1.5 ml of TEA was added dropwise to the solution. The color of the solution rapidly changed from orange to reddish brown, accompanied by appreciable heat release, and the gel was formed. The gel was then completely dried. The dried gel was calcined at 300 °C in an air atmosphere to obtain MIONPs. The powder so prepared was referred to as S-1.

### 2.3. Coating of iron oxide nanoparticles with PEG-6000

For coating MIONPs, PEG solutions with different concentrations were prepared by dissolving PEG-6000 flakes in distilled water. MIONPs were added and mixed with the PEG-6000 solution for 3 hours. The coated particles were dried under an IR lamp. Following the above procedure, four sets of samples were prepared by varying the concentration (5%, 10%, 20% and 30% by weight) of PEG and were respectively referred to as S-5, S-10, S-20, and S-30.

### 2.4. Measurements

The structural characterization of PEG-coated and uncoated  $\text{Fe}_3\text{O}_4$  nanoparticles was carried out using an X-ray diffractometer (Miniflex 600, Rigaku) with  $\text{CuK}\alpha 1$  radiation ( $\lambda = 1.5406 \text{ \AA}$ ). Morphological study of the  $\text{Fe}_3\text{O}_4$  nanoparticles was performed using field emission scanning electron microscopy (FESEM model S4800 type II, Hitachi High Technologies). Quantitative analysis of the  $\text{Fe}_3\text{O}_4$  nanoparticles was carried out using EDAX analysis of the FESEM equipment (model Bruker Nano

GmbH X Flash Detector 5030). Fourier transform infrared spectroscopy (FTIR) of  $\text{Fe}_3\text{O}_4$  nanoparticles was recorded using Spectrum BX (Perkin Elmer) in the range of 600-4000  $\text{cm}^{-1}$ . Thermogravimetric analysis (TGA) study of  $\text{Fe}_3\text{O}_4$  nanoparticles was done by STA-6000 (Perkin Elmer) in the temperature range 50-800 °C under nitrogen atmosphere. Magnetic properties of  $\text{Fe}_3\text{O}_4$  nanoparticles were carried out at room temperature using a vibrating sample magnetometer (VSM EZ9; Microsense Inc., USA).

### 3. Results and discussion

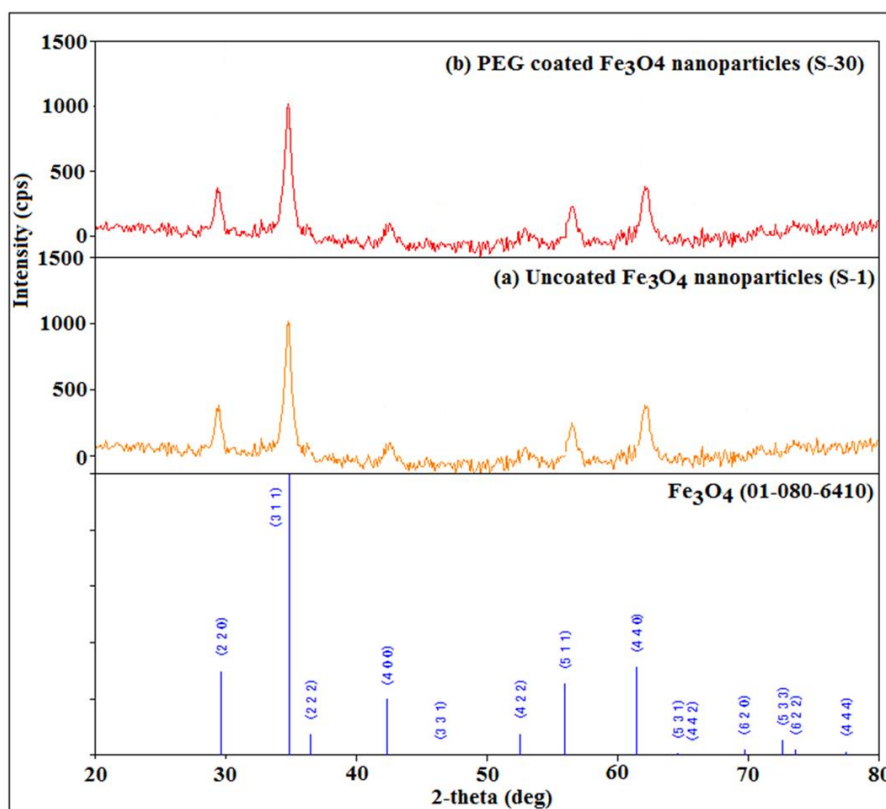
#### 3.1. X-ray Diffraction (XRD) studies

Figure 1 shows the XRD patterns of (a) uncoated and (b) PEG-coated  $\text{Fe}_3\text{O}_4$  nanoparticles. The XRD patterns in Figure 1 (a) and Figure 1 (b) confirmed the nanoparticles to be magnetite ( $\text{Fe}_3\text{O}_4$ ) phase of iron oxide (ICDD Card No. 01-080-6410) with a cubic inverse spinel structure. The average crystallite size of  $\text{Fe}_3\text{O}_4$  nanoparticles was determined using Scherrer's formula  $t=0.94\lambda/B\cos\theta$ , where  $\lambda$  is the wavelength (CuK $\alpha$ 1 radiation  $\lambda=1.5406\text{\AA}$ ), B is the full width at half maximum in radians, and  $\theta$  is

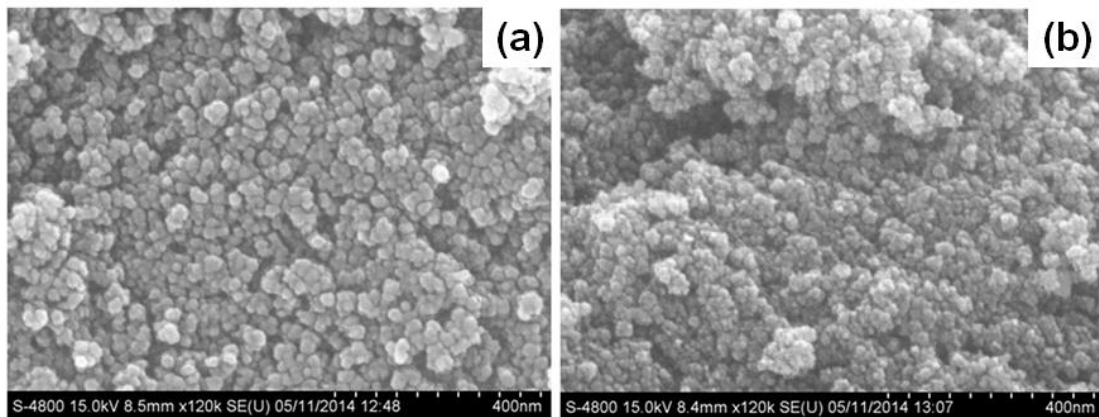
the diffraction angle of the peak [23]. The most prominent peak at  $\theta=35.6^\circ$  was chosen to calculate the average crystallite size. The estimated average size of the  $\text{Fe}_3\text{O}_4$  nanoparticles was found to be 16.2nm.

#### 3.2. Field Emission Scanning Electron Microscopy (FESEM) and EDAX

Figure 2 (a) and (b) indicate the FESEM images of uncoated and PEG-coated  $\text{Fe}_3\text{O}_4$  nanoparticles. These figures reveal that the synthesized  $\text{Fe}_3\text{O}_4$  nanoparticles are approximately spherical in shape. The uncoated  $\text{Fe}_3\text{O}_4$  nanoparticles are agglomerated due to magnetodipole interactions between the  $\text{Fe}_3\text{O}_4$  nanoparticles. After the coating of PEG on the surfaces of  $\text{Fe}_3\text{O}_4$  nanoparticles, the agglomeration of nanoparticles is observed to be minimized [24]. Image blurring in the case of coated  $\text{Fe}_3\text{O}_4$  nanoparticles may be due to the film formation [25]. The surface of the PEG-coated  $\text{Fe}_3\text{O}_4$  nanoparticles seems to be rougher due to the polymerization occurring on the surface of the nanoparticles and strong interfacial interaction between the polymer and  $\text{Fe}_3\text{O}_4$  nanoparticles [26].



**Figure 1.** XRD Patterns of (a) uncoated  $\text{Fe}_3\text{O}_4$  nanoparticles (S-1) and (b) PEG-coated  $\text{Fe}_3\text{O}_4$  nanoparticles (S-30).



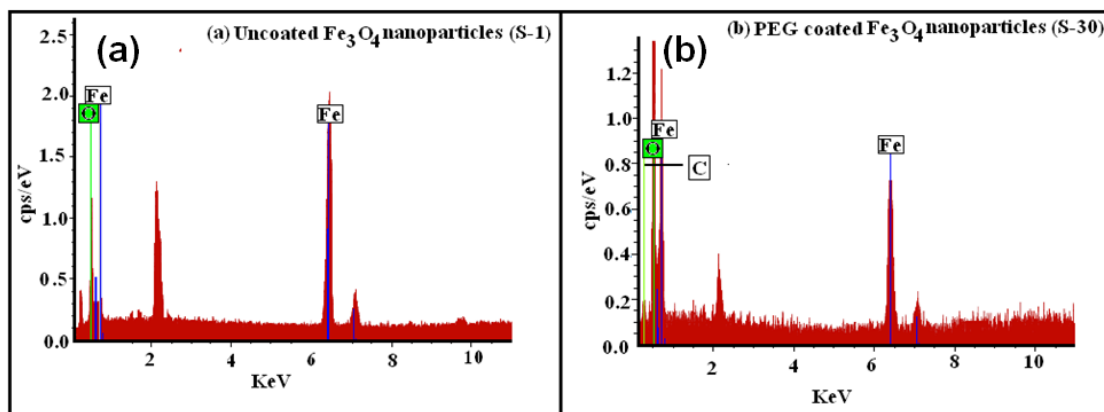
**Figure 2.** FESEM images of (a) uncoated  $\text{Fe}_3\text{O}_4$  nanoparticles (S-1) and (b) PEG-coated  $\text{Fe}_3\text{O}_4$  nanoparticles (S-30).

Figure 3 (a) and (b) present EDAX spectra of uncoated and PEG-coated  $\text{Fe}_3\text{O}_4$  nanocrystalline powders. The spectrum in Figure 3 (a) consists of two peaks related to Fe and O, while Figure 3 (b) includes three peaks related to Fe, O, and C. The peak corresponding to C in Figure 3 (b) may be due to the existence of PEG on the surface of  $\text{Fe}_3\text{O}_4$  nanoparticles. The EDAX technique is unable to detect light elements like H. Therefore, the peak corresponding to H may be absent [27, 28].

### 3.3. Thermo Gravimetric Analysis (TGA)

Curves (a), (b), and (c) in Figure 4 show TGA curves of pure PEG-6000 flakes, uncoated and PEG-coated iron oxide nanocrystalline powder, respectively. It is clear from curve (a) in Figure 4 that there was a weight loss of 2.9% during 50 °C to 340 °C and a weight loss of 95.3%

during 340 °C to 420 °C. The PEG was observed to be completely decomposed at 420 °C. In Figure 4, the curve (b) corresponds to the uncoated  $\text{Fe}_3\text{O}_4$  nanoparticles, which were almost stable, and the weight loss of only 2.4% was seen. This showed that the powder was thermodynamically stable. Curve (c) shows the weight loss of 1.1% in the temperature range 50 °C to 230 °C. But a continuous weight loss of 17.3% was observed in the temperature range of 230 °C to 390 °C. The weight loss may be due to the decomposition of PEG on the surface of  $\text{Fe}_3\text{O}_4$  nanoparticles. At 390 °C, PEG was completely decomposed, and only  $\text{Fe}_3\text{O}_4$  nanoparticles remained. The decomposition temperature of PEG was shifted from 420 °C to 390 °C as indicated in curve (c). It may be because of a change in the chemical environment and oxidative degradation reactions, which can lower the decomposition temperature [29].



**Figure 3.** EDAX spectra of (a) uncoated  $\text{Fe}_3\text{O}_4$  nanoparticles (S-1) and (b) PEG-coated  $\text{Fe}_3\text{O}_4$  nanoparticles (S-30).

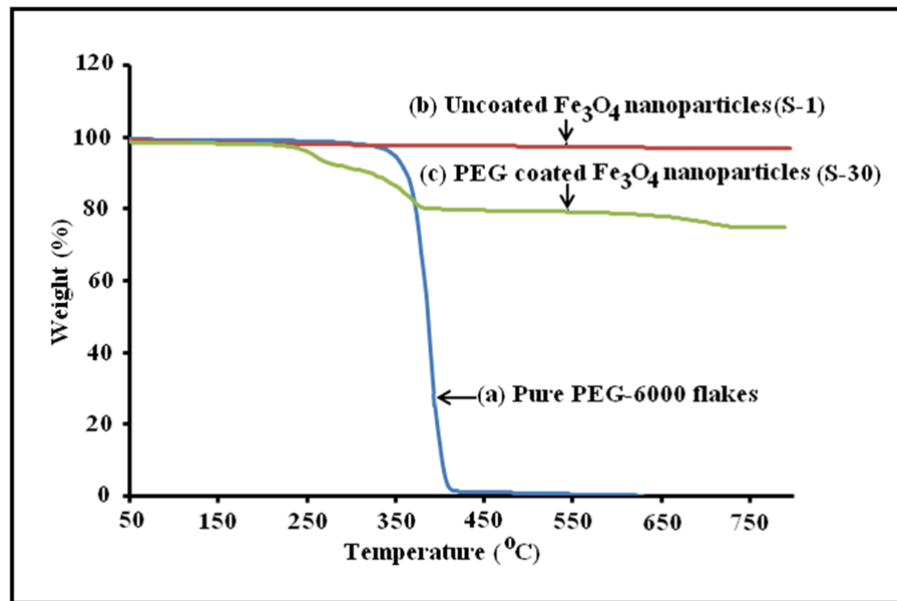


Figure 4. TGA curves of: (a) pure PEG-6000 flakes, (b) uncoated  $\text{Fe}_3\text{O}_4$  nanoparticles (S-1), and (c) PEG-coated  $\text{Fe}_3\text{O}_4$  nanoparticles (S-30).

### 3.4. Fourier Transform Infrared Spectroscopy (FT-IR)

Curves (a), (b), and (c) in Figure 5 show the FT-IR spectrum of uncoated  $\text{Fe}_3\text{O}_4$  nanoparticles, PEG-6000-coated  $\text{Fe}_3\text{O}_4$  nanoparticles, and pure PEG-6000 flakes, respectively. The peak at  $2883.88\text{ cm}^{-1}$  may be attributed to the symmetric stretching of the  $\text{CH}_2$  group [27, 30]. The absorption peak observed at  $2359.65\text{ cm}^{-1}$  may be due to the absorption of atmospheric  $\text{CO}_2$  on the metallic cations [31, 32]. The absorption peak observed around  $1466.01\text{ cm}^{-1}$  in curves in Figure 5 (b) may be caused by

the bending vibration of the C-H bond of the  $\text{CH}_2$  group. The absorption peaks at  $1359.33$ ,  $1340.45$ ,  $1278.27$ ,  $1240.05$ ,  $1142.75$ ,  $1100.65$ ,  $1060.03\text{ cm}^{-1}$  in curves (b) and (c) may result from the bending vibration of the O-H bond and stretching vibration of the C-O bond of the  $-\text{CH}_2-\text{OH}$  group [33, 34].

The strong absorption peak at  $1100.41\text{ cm}^{-1}$  in curve (b) and  $1100.65\text{ cm}^{-1}$  in curve (c) may be attributed to the  $-\text{CH}_2-\text{O}-\text{CH}_2-$  group of PEG-6000. The presence of  $\text{CH}_2-\text{O}-\text{CH}_2$ ,  $-\text{CH}_2$ , and  $-\text{CH}$  peaks in the spectrum of coated

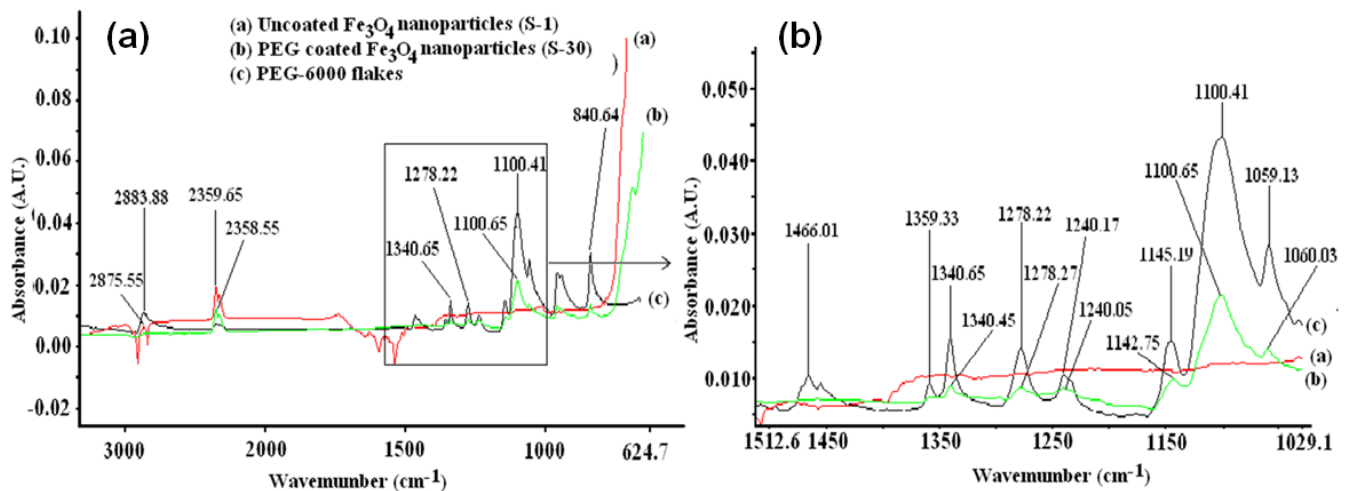
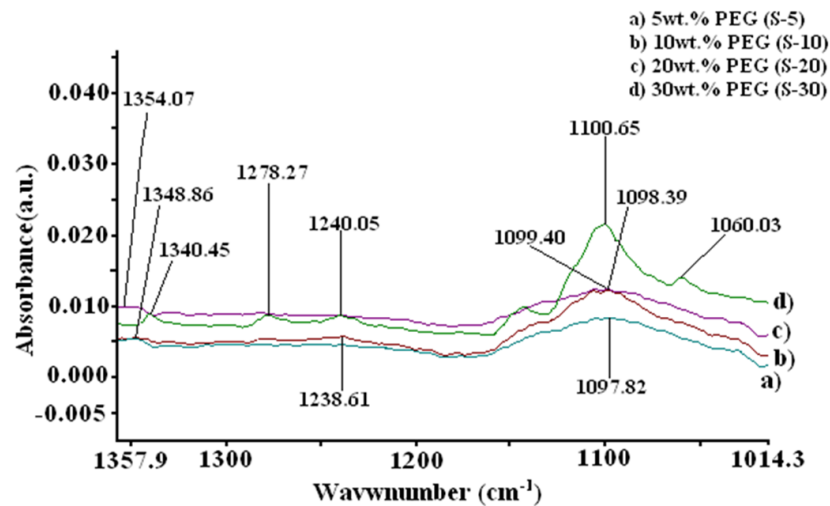


Figure 5. FT-IR spectra (a) and results in a selected wavenumber area (b) of uncoated  $\text{Fe}_3\text{O}_4$  nanoparticles (S-1, curve a), PEG-coated  $\text{Fe}_3\text{O}_4$  nanoparticles (S-30, curve b), and pure PEG-6000 (curve c).



**Figure 6.** FT-IR spectra of  $\text{Fe}_3\text{O}_4$  nanoparticles coated with (5-30wt %) of PEG.

powder, as shown in Figure 5 (b), may be due to PEG-6000 covering on the surface of  $\text{Fe}_3\text{O}_4$  nanoparticles. The above results suggest that the nanoparticles associated with iron oxide powder were successfully coated by PEG [35].

Curves (a), (b), (c), and (d) in Figure 6 represent FT-IR spectra of  $\text{Fe}_3\text{O}_4$  nanoparticles coated with 5 wt % , 10wt % , 20wt% , and 30wt% PEG, respectively. The FT-IR spectra consist of strong and well-defined bands around  $1100\text{ cm}^{-1}$ . It is clear from Fig. 6(a-d) that the

height of the absorption peak ( $1100\text{ cm}^{-1}$ ) increases with the increase of PEG content. It may be due to a larger quantity of hydroxyl group ( $-\text{CH}_2\text{-O-CH}_2-$ ) bonding to the  $\text{Fe}_3\text{O}_4$  nanoparticles [36].

### 3.5. Magnetization

Figure 7 (a) and (b) show the simple laboratory experiment with a bar magnet to demonstrate the magnetic nature of the  $\text{Fe}_3\text{O}_4$  nanoparticles using a bar magnet. In the absence of a bar magnet,  $\text{Fe}_3\text{O}_4$

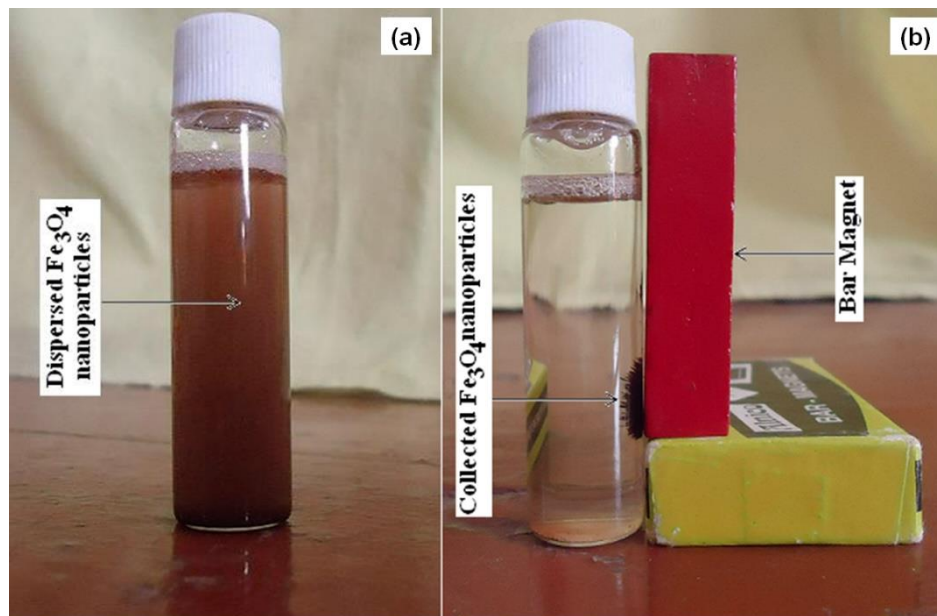


**Figure 7.** (a) Dispersed nanoparticles in the absence of a bar magnet and (b) collection of nanoparticles in the presence of a bar magnet.

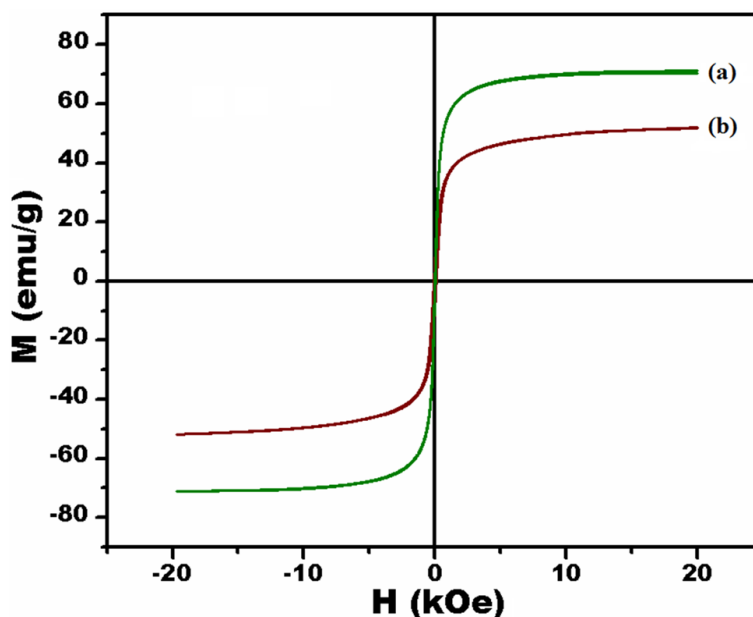


**Figure 8.** Magnetization curves for (a)  $\text{Fe}_3\text{O}_4$  nanoparticles (S-1) and (b) PEG-coated  $\text{Fe}_3\text{O}_4$  nanoparticles (S-30).

nanoparticles were observed to be dispersed uniformly in solution, as indicated in Figure 7 (a). In the presence of a bar magnet,  $\text{Fe}_3\text{O}_4$  nanoparticles were observed to be collected toward the bar magnet as shown in Figure 7(b). Due to their magnetic nature,  $\text{Fe}_3\text{O}_4$  nanoparticles were observed to gather near the magnet [28, 37, 38].

The magnetic properties of uncoated and PEG-coated  $\text{Fe}_3\text{O}_4$  nanoparticles were studied at room temperature by the vibrating sample magnetometer (VSM), as shown in Figure 8. From Figure 8, it can be seen that the magnetization curves appeared to be S-shaped over the applied field from -20 to +20 kOe. The uncoated and PEG-coated  $\text{Fe}_3\text{O}_4$  nanoparticles exhibit excellent superparamagnetic behavior with zero coercivity and high saturation magnetization. The saturation magnetization ( $M_s$ ) for uncoated and PEG-coated  $\text{Fe}_3\text{O}_4$  nanoparticles was found to be 71 emu/g and 51 emu/g, respectively. The value of saturation magnetization of PEG-coated  $\text{Fe}_3\text{O}_4$  nanoparticles is lower than that of uncoated  $\text{Fe}_3\text{O}_4$  nanoparticles. This may be due to the existence of PEG. For biomedical applications, it is required that  $\text{Fe}_3\text{O}_4$  nanoparticles should be monodisperse in nature, superparamagnetic with high saturation magnetization. Therefore, the PEG-coated  $\text{Fe}_3\text{O}_4$  nanoparticles may be promising candidates for biomedical applications, such as hyperthermia treatment, magnetic resonance imaging, etc. [39-43].

#### 4. Conclusions

PEG-coated  $\text{Fe}_3\text{O}_4$  nanoparticles were synthesized by a simple, cost-effective sol-gel method by optimizing experimental conditions. The structural, morphological, and thermal properties of PEG-coated  $\text{Fe}_3\text{O}_4$  nanoparticles were studied using different techniques. Coating of PEG on the surface of  $\text{Fe}_3\text{O}_4$  nanoparticles was confirmed by FT-IR spectroscopy. As the concentration of PEG increases, the absorbance also increases. PEG-coated  $\text{Fe}_3\text{O}_4$  nanoparticles were observed to be superparamagnetic in nature and also exhibit high saturation magnetization. Therefore, the PEG-coated  $\text{Fe}_3\text{O}_4$  nanoparticles may be promising for biomedical applications.

#### Acknowledgments

Authors are heartily thankful to Rashtriya Uchcharat Shiksha Abhiyan (RUSA) MHRD, New Delhi, for financial support. The authors would also like to thank the Head of Physics Department and Principal Pratap College, Amalner, Dist: Jalgaon, Maharashtra, for providing laboratory facilities.

## Conflict of Interest

The authors declare no conflict of interest.

## References

1. L.S. Ganapathe, et al. Magnetite (Fe<sub>3</sub>O<sub>4</sub>) Nanoparticles in Biomedical Application: From Synthesis to Surface Functionalisation. *Magnetochemistry*, 2020, 6, 68.
2. C. Vincent, et al. Iron Oxide Nanoparticles: Types, Synthesis, Biomedical applications and Scope of Nanoinformatics. *Biological Forum – An International Journal*, 2023, 15, 927.
3. M.L. López-Moreno, et al. Environmental behavior of coated NMs: Physicochemical aspects and plant interactions. *Journal of Hazardous Materials*, 2018, 347, 196.
4. M.E.A. El-sayed. Nanoadsorbents for water and wastewater remediation. *Science of The Total Environment*, 2020, 739, 139903.
5. S. Matsuo, S. Kobayashi, and K. Ono. Magnetization process of concave Fe<sub>3</sub>O<sub>4</sub> nanoparticles. *Journal of Physics and Chemistry of Solids*, 2026, 208, 113020.
6. L. Peixoto, et al. Magnetic nanostructures for emerging biomedical applications. *Applied Physics Reviews*, 2020, 7, 011310.
7. Y. Yan, et al. Morphology-dependent magnetic hyperthermia characteristics of Fe<sub>3</sub>O<sub>4</sub> nanoparticles. *Materials Chemistry and Physics*, 2025, 329, 130045.
8. D.L. Pérez, et al. Synthesis of superparamagnetic iron oxide nanoparticles coated with polyethylene glycol as potential drug carriers for cancer treatment. *Journal of Nanoparticle Research*, 2024, 26, 2.
9. J.E. Ogbezode, et al. A narrative review of the synthesis, characterization, and applications of iron oxide nanoparticles. *Discover Nano*, 2023, 18, 125.
10. F. Chang and G.-L. Davies. From 0D to 2D: Synthesis and bio-application of anisotropic magnetic iron oxide nanomaterials. *Progress in Materials Science*, 2024, 144, 101267.
11. B. Thapa, et al. Enhanced MRI T<sub>2</sub> Relaxivity in Contrast-Probed Anchor-Free PEGylated Iron Oxide Nanoparticles. *Nanoscale Research Letters*, 2017, 12, 312.
12. G. Antarnusa and E. Suharyadi. A synthesis of polyethylene glycol (PEG)-coated magnetite Fe<sub>3</sub>O<sub>4</sub> nanoparticles and their characteristics for enhancement of biosensor. *Materials Research Express*, 2020, 7, 056103.
13. G. Antarnusa, et al. The Effect of Additional Polyethylene Glycol (PEG) as Coating Fe<sub>3</sub>O<sub>4</sub> for Magnetic Nanofluid Applications. *Recent Innovations in Chemical Engineering (Formerly Recent Patents on Chemical Engineering)*, 2021, 14, 335.
14. S. Arsalani, et al. Uniform size PEGylated iron oxide nanoparticles as a potential theranostic agent synthesized by a simple optimized coprecipitation route. *Journal of Magnetism and Magnetic Materials*, 2022, 564, 170091.
15. C. Ravikumar. Unveiling the formation mechanism of polydisperse iron oxide nanoparticles in coprecipitation route. *Journal of Crystal Growth*, 2023, 624, 127419.
16. C. Zhang and I. Zhitomirsky. Hydrothermal synthesis of iron oxides in the presence of catecholate capping agent for supercapacitor electrodes. *Materials Letters*, 2025, 401, 139229.
17. I. Karimzadeh, H.R. Dizaji, and M. Aghazadeh. Development of a facile and effective electrochemical strategy for preparation of iron oxides (Fe<sub>3</sub>O<sub>4</sub> and γ-Fe<sub>2</sub>O<sub>3</sub>) nanoparticles from aqueous and ethanol mediums and in situ PVC coating of Fe<sub>3</sub>O<sub>4</sub> superparamagnetic nanoparticles for biomedical applications. *Journal of Magnetism and Magnetic Materials*, 2016, 416, 81.
18. A. Ullrich, et al. Synthesis of iron oxide nanoparticles by decomposition of iron-oleate: influence of the heating rate on the particle size. *Journal of Nanoparticle Research*, 2022, 24, 183.
19. L. Durães, et al. Phase investigation of as-prepared iron oxide/hydroxide produced by sol-gel synthesis. *Materials Letters*, 2005, 59, 859.
20. L. Durães, et al. Characterization of iron(III) oxide/hydroxide nanostructured materials produced by sol-gel technology based on the Fe(NO<sub>3</sub>)<sub>3</sub>·9H<sub>2</sub>O–C<sub>2</sub>H<sub>5</sub>OH–CH<sub>3</sub>CH<sub>2</sub>O system. *Materials Chemistry and Physics*, 2011, 130, 548.
21. M. Anuje, et al. Synthesis, Characterization, and Cytotoxicity Evaluation of Polyethylene Glycol-Coated Iron Oxide Nanoparticles for Radiotherapy Application. *Journal of Medical Physics*, 2021, 46, 154.
22. V. Patsula, et al. Size-dependent magnetic properties of iron oxide nanoparticles. *Journal of Physics and Chemistry of Solids*, 2016, 88, 24.
23. A.E. Eken and M. Ozenbas. Characterization of nanostructured magnetite thin films produced by sol-gel processing. *Journal of Sol-Gel Science and Technology*, 2009, 50, 321.
24. D.-L. Zhao, et al. Magnetic and inductive heating properties of Fe<sub>3</sub>O<sub>4</sub>/polyethylene glycol composite nanoparticles with core-shell structure. *Journal of Alloys and Compounds*, 2010, 502, 392.
25. A. Petri-Fink, et al. Effect of cell media on polymer coated superparamagnetic iron oxide nanoparticles (SPIONs): Colloidal stability, cytotoxicity, and cellular uptake studies. *European Journal of Pharmaceutics and Biopharmaceutics*, 2008, 68, 129.

26. H. Gu, et al. Magneto-resistive polyaniline-magnetite nanocomposites with negative dielectrical properties. *Polymer*, **2012**, 53, 801.
27. A. Mukhopadhyay, et al. A Facile Synthesis of PEG-Coated Magnetite (Fe<sub>3</sub>O<sub>4</sub>) Nanoparticles and Their Prevention of the Reduction of Cytochrome C. *ACS Applied Materials & Interfaces*, **2011**, 4, 142.
28. M. Mahdavi, et al. Synthesis, Surface Modification and Characterisation of Biocompatible Magnetic Iron Oxide Nanoparticles for Biomedical Applications. *Molecules*, **2013**, 18, 7533.
29. K. Król-Morkisz and K. Pielichowska, *Thermal Decomposition of Polymer Nanocomposites With Functionalized Nanoparticles*, in *Polymer Composites with Functionalized Nanoparticles*. **2019**, Elsevier. p. 405.
30. Y.F. Shen, et al. Preparation and application of magnetic Fe<sub>3</sub>O<sub>4</sub> nanoparticles for wastewater purification. *Separation and Purification Technology*, **2009**, 68, 312.
31. S. Maensiri, et al. Synthesis and optical properties of nanocrystalline V-doped ZnO powders. *Optical Materials*, **2007**, 29, 1700.
32. C.C. Vidyasagar, et al. Optical Properties of Dye-Sensitized Films Based on Cd-ZnO Nanoparticles. *Nanoscience and Nanotechnology: An International Journal*, **2012**, 2, 18.
33. H. Matsuura and T. Miyazawa. Vibrational analysis of molten poly(ethylene glycol). *Journal of Polymer Science Part A-2: Polymer Physics*, **1969**, 7, 1735.
34. C. Barrera, A.P. Herrera, and C. Rinaldi. Colloidal dispersions of monodisperse magnetite nanoparticles modified with poly(ethylene glycol). *Journal of Colloid and Interface Science*, **2009**, 329, 107.
35. C.I. Covaliu, et al. Core-shell hybrid nanomaterials based on CoFe<sub>2</sub>O<sub>4</sub> particles coated with PVP or PEG biopolymers for applications in biomedicine. *Powder Technology*, **2013**, 237, 415.
36. L.T.M. Hoa, et al. Preparation and characterization of magnetic nanoparticles coated with polyethylene glycol. *Journal of Physics: Conference Series*, **2009**, 187, 012048.
37. J. Drbohlavova, et al. Preparation and Properties of Various Magnetic Nanoparticles. *Sensors*, **2009**, 9, 2352.
38. E. Darezereshki, M. Ranjbar, and F. Bakhtiari. One-step synthesis of maghemite (γ-Fe<sub>2</sub>O<sub>3</sub>) nano-particles by wet chemical method. *Journal of Alloys and Compounds*, **2010**, 502, 257.
39. T. Ozkaya, et al. Synthesis of Fe<sub>3</sub>O<sub>4</sub> nanoparticles at 100°C and its magnetic characterization. *Journal of Alloys and Compounds*, **2009**, 472, 18.
40. P.B. Santhosh and N.P. Ulrih. Multifunctional superparamagnetic iron oxide nanoparticles: Promising tools in cancer theranostics. *Cancer Letters*, **2013**, 336, 8.
41. S. García-Jimeno and J. Estelrich. Ferrofluid based on polyethylene glycol-coated iron oxide nanoparticles: Characterization and properties. *Colloids and Surfaces A: Physicochemical and Engineering Aspects*, **2013**, 420, 74.
42. L. Dai, et al. One-pot facile synthesis of PEGylated superparamagnetic iron oxide nanoparticles for MRI contrast enhancement. *Materials Science and Engineering: C*, **2014**, 41, 161.
43. M. Anbarasu, et al. Synthesis and characterization of polyethylene glycol (PEG) coated Fe<sub>3</sub>O<sub>4</sub> nanoparticles by chemical co-precipitation method for biomedical applications. *Spectrochimica Acta Part A: Molecular and Biomolecular Spectroscopy*, **2015**, 135, 536.

---

© 2025 The Authors. This article is licensed under a Creative Commons Attribution 4.0 BY International License. 